ELSEVIER

Surface Science 442 (1999) 65–73

surface science

www.elsevier.nl/locate/susc

Si(111)-($\sqrt{3}\times\sqrt{3}$)-Ag surface at low temperatures: symmetry breaking and surface twin boundaries

N. Sato [a], T. Nagao [a,b], S. Hasegawa [a,b,*]

[a] *Department of Physics, Graduate School of Science, University of Tokyo, 7-3-1 Hongo, Bunkyo-ku, Tokyo 113-0033, Japan*
[b] *Core Research for Evolutional Science and Technology, The Japan Science and Technology Corporation, Kawaguchi Center Building, Hon-cho 4-1-8, Kawaguchi, Saitama 332-0012, Japan*

Received 1 March 1999; accepted for publication 6 July 1999

Abstract

In contrast to the honeycomb pattern observed at room temperature in empty-state scanning-tunneling-microscopy (STM) images corresponding to the generally accepted honeycomb-chained-triangle (HCT) structure, the Si(111)-($\sqrt{3}\times\sqrt{3}$)-Ag surface at low temperatures (62 and 6 K) shows a hexagonal-lattice pattern. This is consistent with an 'inequivalent-triangle (IET) model' recently proposed as the most stable structure for the ($\sqrt{3}\times\sqrt{3}$)-Ag surface in which two Ag triangles in the unit cell are different in size. Because of the asymmetry of the IET structure, two types of domains whose structures are in the relation of twins to each other are created only at low temperatures, between which surface twin boundaries (TB) appear. The neighboring domains, separated by a conventional out-of-phase boundary (OPB), tend to have the IET structures of the opposite symmetry. The interaction between the OPB and TB is discussed. The TB is observed to fluctuate and to be pinned by some defects.

Keywords: Scanning tunneling microscopy; Scanning tunneling spectroscopies; Silicon; Silver; Surface defects; Surface relaxation and reconstruction; Surface structure, morphology, roughness, and topography

1. Introduction

The honeycomb-chained-triangle (HCT) model [1,2] is now widely accepted as an atomic structure of the Si(111)-($\sqrt{3}\times\sqrt{3}$)-Ag surface after much experimental and theoretical investigation. Today, no one seems to cast any doubt upon this structural model.

Recently, Aizawa et al. performed first-principles calculations with a structural optimization upon the ($\sqrt{3}\times\sqrt{3}$)-Ag structure again, and found a more stable atomic arrangement than the HCT model, which was named inequivalent-triangle (IET) model as shown in Fig. 1a [3]. This structure is almost the same as the HCT structure, but the Si trimers (filled circles) are twisted by 6° compared to the HCT model. As a result of this twist, one of the two Ag triangles (large open circles connected with dashed lines) in the ($\sqrt{3}\times\sqrt{3}$) unit cell becomes larger, and the other becomes smaller. So the mirror-plane along the [$1\bar{2}1$] direction in the HCT model disappears in the IET model. The HCT structure belongs to the space group of *p31m* whereas the IET structure to that of *p3*. According to the theoretical calculations [3], the difference in size between the two Ag triangles in the unit cell

* Corresponding author. Fax: +81-3-5841-4167.
E-mail address: shuji@surface.phys.s.u-tokyo.ac.jp (S. Hasegawa)

0039-6028/99/$ – see front matter
PII: S0039-6028(99)00856-0

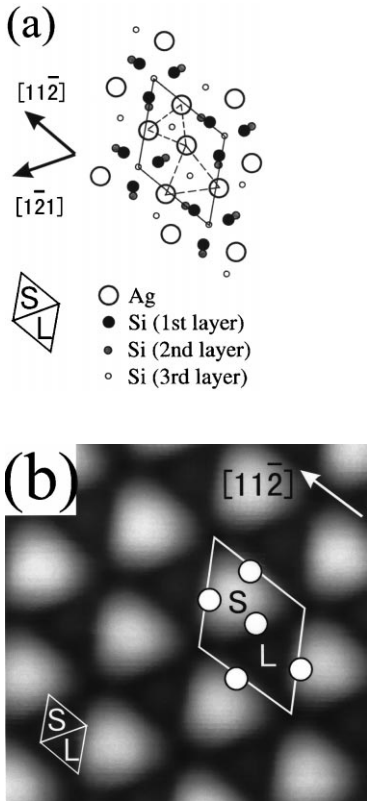

Fig. 1. (a) A schematic illustration of the IET model for the atomic structure of the Si(111)-($\sqrt{3}\times\sqrt{3}$)-Ag surface (from Ref. [3]). —, The unit cell; - - -, chained Ag triangles; ●, first-layer Si atoms forming the Si trimers. (b) An empty-state STM image of the Si(111)-($\sqrt{3}\times\sqrt{3}$)-Ag surface at 6 K taken in constant-current mode. The image size is 21 Å × 21 Å with the sample bias voltage $V_s = 0.9$ V and tunneling current of $I =$ 1.5 nA. —, The unit cell; ○, positions of the Ag atoms. The S- and L-halves are also shown schematically.

makes a difference in apparent height in the empty-state scanning-tunneling-microscopy (STM) images. Therefore a honeycomb pattern of the HCT structures at room temperature (RT) becomes a hexagonal-lattice pattern which was actually observed by STM at low temperature (LT) [3]. Since there are two ways of twisting the Si trimer (clockwise and anticlockwise), two types of structures in a twin relation exist. And two types of domains consisting of each twin meet to make domain boundaries. Such surface twin boundaries (TB) were reported in the previous study [3].

In this paper, we present more detailed investigations of the IET structure and TB of the ($\sqrt{3}\times\sqrt{3}$)-Ag surface at low temperatures. The existence of such twin domains must conversely prove the validity of the IET structure itself, but is not an artifact caused by some tip-shape effect such as shown in a theoretical calculation [4]; some peculiar tip shapes may distort the regular honeycomb pattern into other patterns including hexagonal-lattice pattern. The most stable structure near the conventional out-of-phase boundary (OPB) [5–7] is found, and the relation between the TB and OPB is discussed. We also succeeded in observing the fluctuating IET domain, which showed a conversion from one of the twin to the other one in the IET structure.

2. Experimental

We used a commercial ultra-high vacuum low-temperature STM (UNISOKU USM501 type) in which the sample could be cooled down to 62 K with supercooled liquid nitrogen or 6 K with liquid helium. The reflection high-energy electron diffraction (RHEED) system equipped with this STM could monitor the surface structure during the sample preparation. The base pressure in the chambers was $< 1\times10^{-10}$ Torr. The substrate was an n-type Si(111) wafer with 0.005 Ωcm resistivity at RT. An electrochemically etched polycrystalline tungsten tip followed by the electron bombardment cleaning in situ was used.

After the clean 7×7 surface was obtained by flashing the sample at 1200°C several times, ca 1 ML (1 monolayer) of Ag was deposited on the Si substrate kept at ca 500°C to prepare the ($\sqrt{3}\times\sqrt{3}$)-Ag surface. Then the sample was transferred to the STM stage that had been already cooled down. We waited several hours to avoid thermal drift, then performed STM observations.

3. Results

3.1. IET structure

A typical empty-state STM image of the ($\sqrt{3}\times\sqrt{3}$)-Ag surface is shown in Fig. 1b, taken

at 6 K. The size is 21 Å × 21 Å and the sample bias voltage is 0.9 V. The unit cell contains two triangles, one is brighter and the other is darker. The theoretical calculation [3] shows that the darker one corresponds to the larger Ag triangle, and the brighter one to the smaller triangle in Fig. 1a. We call the half unit of the $(\sqrt{3}\times\sqrt{3})$-Ag cell with a smaller Ag triangle the S-half and the other half with a larger Ag triangle the L-half as shown in Fig. 1b.

In Fig. 2, two series of bias dependent images of the $(\sqrt{3}\times\sqrt{3})$-Ag surface at RT (Fig. 2a and e) and 62 K (Fig. 2f and j) are displayed. Especially in the empty-state images such as Fig. 2a and f, the difference between a honeycomb pattern at RT and a hexagonal-lattice pattern at 62 K is clearly seen, while in the filled-state images such as Fig. 2e and j, the images are almost the same irrespective of temperature. Though the STM image taken at RT such as Fig. 2d shows a slightly asymmetric pattern, the asymmetric feature is much more prominent at 62 K. Such a slight asymmetric honeycomb pattern at RT has been mentioned in a previous study [8], and it was attributed to the artifact due to the tip shape [4].

Since the filled-state STM images change drastically around $V_S \sim -1.0$ V (Fig. 2d and e or i and j, at the respective temperatures) which is close to the binding energies of the S_2 and S_3 surface states measured in photoemission spectroscopy [9–12], the changes of the images may be attributed to probing those states superimposed on the S_1 state which locates near the Fermi level (E_F). In fact, the theoretical calculation shows that the S_1 state stems mostly from Ag 5p orbitals, while the S_2 and S_3 states come mainly from Ag 5s orbitals [13]. Such different characters with respect to the Ag orbitals may explain the different patterns of the STM images.

In Fig. 3, spectra in scanning tunneling spectroscopy (STS) are shown taken at RT (Fig. 3a) and 62 K (Fig. 3b). Roughly speaking, the STS spectrum Fig. 3a at RT is consistent with the previously reported STS spectra [14–16]. There is a plateau ranging from ca −0.3 eV to the upper empty state (with respect to E_F). The $(\sqrt{3}\times\sqrt{3})$-Ag surface has a dispersive surface state, called S_1,

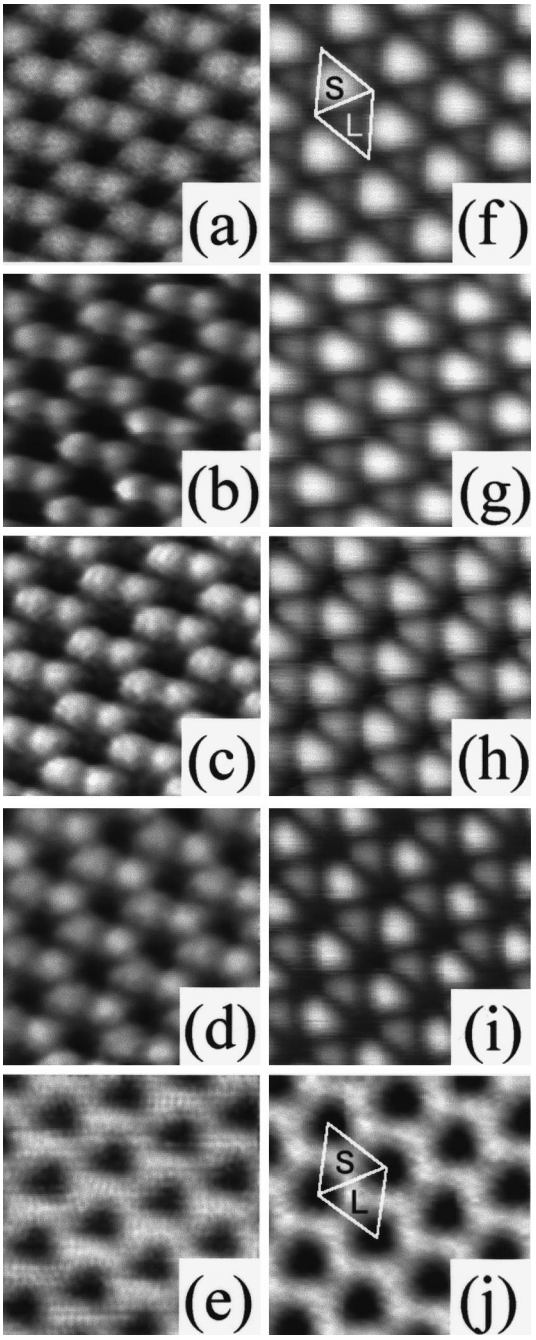

Fig. 2. Two series of STM images of the $(\sqrt{3}\times\sqrt{3})$-Ag surface at RT (a and e) and 62 K (f and j) with the size of 24 Å × 24 Å. (a) $V_s = 1.0$ V, $I = 0.3$ nA; (b) $V_s = 0.6$ V, $I = 0.15$ nA; (c) $V_s = -0.75$, $I = 0.75$ nA; (d) $V_s = -1.0$ V, $I = 0.2$ nA; (e) $V_s = -2.0$ V, $I = 0.8$ nA; (f) $V_s = 1.0$ V, $I = 0.18$ nA; (g) $V_s = 0.5$, $I = 0.2$ nA; (h) $V_s = 0.1$V, $I = 0.18$ nA; (i) $V_s = -0.5$ V, $I = 0.5$ nA; (j) $V_s = -1.0$ V, $I = 2.0$ nA. In (f) and (j), the unit cells are shown with solid lines, and each of them consists of the S-half and L-half.

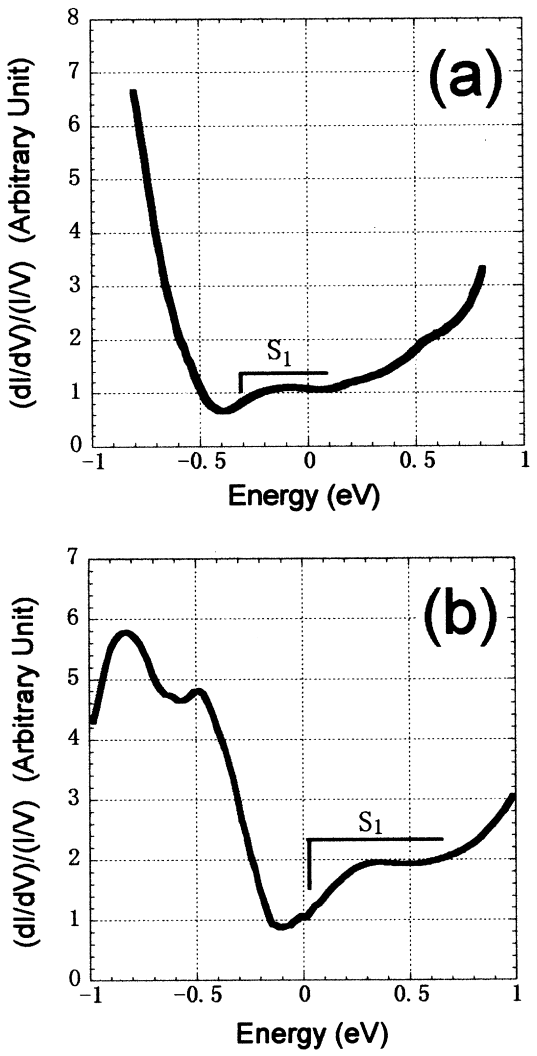

Fig. 3. STS spectra of the $(\sqrt{3}\times\sqrt{3})$-Ag surface (a) at RT and (b) at 62 K. The values $(dI/dV)/(I/V)$ were calculated numerically from the measured I–V curves. Positive energy corresponds to the empty states, and the negative to the filled states.

within the bulk band gap near E_F [3,9–11,17]. Since this is a two-dimensional free-electron like surface state, its density of states is nearly constant, independent of energy. The plateau in the STS spectrum corresponds to this S_1 state, which is also seen in the inverse photoemission study [16] and theoretical calculations [17–20]. The bottom of the S_1 state in Fig. 3a is located at ca 0.2 eV below E_F, which is consistent with the previous photoemission [9–12] and STS [15] studies. But this is inconsistent with the theoretical calculation of energy bands based on the HCT structure [3,17], in which the bottom of the S_1 band locates just at E_F [3], or well above E_F [17].

The shape of the STS spectrum at 62 K shown in Fig. 3b is slightly different from that at RT (Fig. 3a); the plateau corresponding to the S_1-state band is ranging only above E_F. Such an energy position of the S_1-state bottom is consistent with its energy dispersion obtained by the electron standing waves at 6 K [21]. The difference in the energy position of the S_1-state band between at RT (Fig. 3a) and at 62 K (Fig. 3b) may result from an extrinsic reason, that is, Ag adatom gas phase on top of the $(\sqrt{3}\times\sqrt{3})$-Ag surface only at RT [22,23].

The extra Ag atoms after the completion of the $(\sqrt{3}\times\sqrt{3})$-Ag surface exist as a gas phase diffusing on top of this surface [22]. These diffusing Ag atoms come to nucleate and rest at low temperatures and can be observed with our STM, which will be discussed in detail elsewhere [24]. Such a two-dimensional adatom gas phase at RT dopes electrons into the S_1-state band, which shifts the band downward [23]. This extrinsic effect may explain why the onset of the S_1 state in the STS spectra in Fig. 3 changes depending on the temperature, and also why the onset of the S_1 state at RT (Fig. 3a) is different from those in the theoretical calculations on the HCT structure [3,17].

In Fig. 3b, the peak ca $-0.4\sim-0.9$ eV below E_F was observed to split. This may correspond to the split of the S_2 state and S_3 state at the $\bar{K}$ point in the surface Brillouin zone due to the symmetry-breaking in the IET structure [3]. This should be confirmed by low-temperature photoemission spectroscopy.

At low temperatures, almost the whole surface of the $(\sqrt{3}\times\sqrt{3})$-Ag structure shows the hexagonal-lattice pattern, that is, the IET structure in the unit cell, as described so far. But there are a few exceptions. One exception is the honeycomb pattern observed at boundary regions between the adjacent domains in a twin relation each other, which will be explained in the next subsection. Another exception is the structure near the step

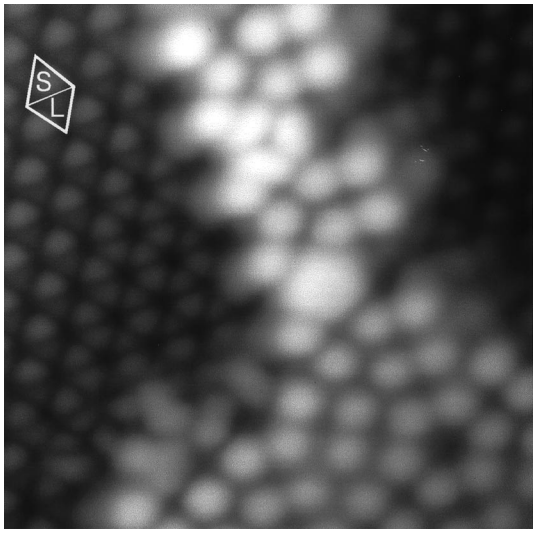

Fig. 4. An empty-state STM image taken at 62 K in the constant-current mode (78 Å × 78 Å). The sample bias voltage is 1.5 V and the tunneling current is 1.3 nA.

edges. In Fig. 4, there remains debris of the 7×7 domains with one step higher than the $(\sqrt{3}\times\sqrt{3})$-Ag domain. Near the bay-shaped step edge of the 7×7 domain, the $(\sqrt{3}\times\sqrt{3})$-Ag surface shows a honeycomb pattern, while it shows a hexagonal-lattice pattern at the regions far away from the 7×7 domain edge. In our STM experiments at low temperatures, the honeycomb pattern showing the HCT structure are observed only in such special cases.

3.2. Domain boundaries

At RT, the $(\sqrt{3}\times\sqrt{3})$-Ag surface consists of the HCT structure. During cooling down the sample below RT, the HCT structure goes into the IET structure, so that the surface is split into two types of domains in a twin relation because of its asymmetry in structure. Here, we introduce a definition to identify the two types of domains of the IET structure in a relation of twins. The Si trimers of the first layer in the IET structure are twisted (by 6° according to the theoretical calculation [3]) compared to those of the HCT structure. There are two ways of twisting the Si trimers, clockwise and anticlockwise. For the domains where the Si trimers are twisted anticlockwise, we

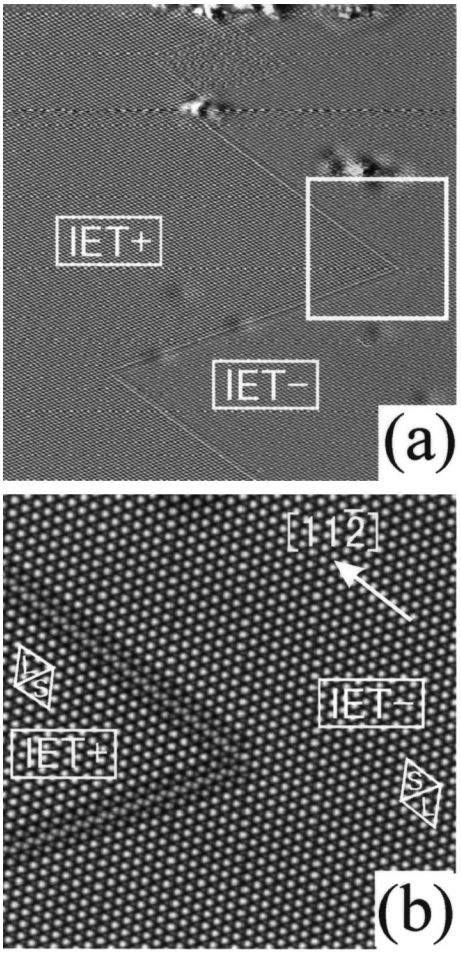

Fig. 5. (a) An empty-state STM image taken at 6 K in the constant-height mode ($V_s=1.0$ V, $I=0.5$ nA, 840 Å × 800 Å). (b) A magnified image of the square area in (a) taken at 6 K in the constant-current mode ($V_s=1.0$ V, $I=0.5$ nA, 245 Å × 245 Å).

call IET+ domains, while the IET− domains have the IET structure with Si trimers twisted clockwise. Then the atomic arrangement in Fig. 1a is the IET− structure, and the domain observed in Fig. 1b is also classified as the IET− domain. So, the boundaries between the IET+ and IET− domains are formed through this symmetry-breaking process during cooling down. Such a surface TB is shown in Fig. 5 taken at 6 K.

In Fig. 5a, there is a straight line running in the ⟨112⟩ directions, but sharply bent 60°. The magnified image of Fig. 5a is shown in Fig. 5b. The left domain is the IET+ domain, while the right

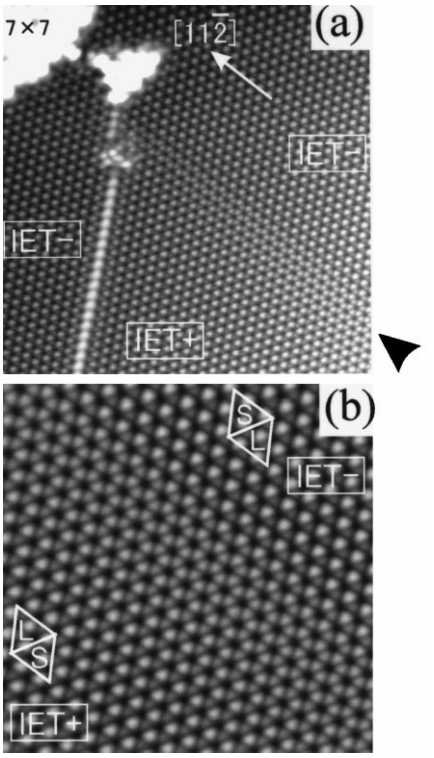

Fig. 6. STM images with a type-I OPB and a TB taken at 62 K in the constant-current mode with $V_s = 1.5$ V and $I = 1.3$ nA. The sizes are (a) 140 Å × 140 Å and (b) 115 Å × 115 Å. The left upper corner in (a) is the 7 × 7 domain which becomes bright because of contrast enhancement, and the adjacent small bright domain is a defect. The TB is running from near the defect to the arrowhead shown out of the image.

domain is the IET− domain. A straight TB is formed between these domains. At the boundary, the $(\sqrt{3} \times \sqrt{3})$-Ag structure shows rather a honeycomb pattern. A domain boundary in the previous report [21] (called type-Ib there) was this TB, at which electron standing waves were not formed.

A bright straight line running along [$\bar{2}$11] direction to the lower left in Fig. 6a is seen, which is a conventional out-of-phase domain boundary (OPB, called type-I) [5–7]. The domains of the respective sides of the OPB are always formed to have the opposite symmetry; the left-side domain is the IET− domain, while the right is the IET+ one. This configuration of the twin domains at the OPB seems to be energetically favorable. The OPBs are formed during the deposition of Ag to prepare the $(\sqrt{3} \times \sqrt{3})$-Ag structure at 500°C. Since the both sides of the OPB have the same HCT structure at RT, the HCT structure changes into the IET structure below RT, resulting in the splitting into the IET+ and IET− domains during cooling. From a defect at this OPB seen at the upper in this image, a TB is running in the direction of [11$\bar{2}$] towards the lower right as indicated by an arrowhead. This TB region is wider than that in Fig. 5. The region of the TB is magnified in Fig. 6b. The hexagonal-lattice pattern in the lower left IET+ domain changes gradually into the other hexagonal-lattice pattern in the upper right IET− domain through the TB region showing the honeycomb pattern.

In Fig. 7a, a semicircular TB, originating from the both edges of the OPB, is formed passing through a defect (indicated by A). Also in this image, the IET domains arrange in the most stable way; the right side and the left side of the OPB have the opposite IET symmetry. During the scan, a contamination from the tip fell down at the right of the OPB indicated by B in Fig. 7b. The existence of the contamination changed the arrangement of the semicircular TB; the TB are unpinned from the defect A and newly pinned by the contamination B. While scanning the same area after taking the image (Fig. 7b), the semicircular TB in Fig. 7b sometimes disappeared as shown in Fig. 7c and appeared again in the same configuration as Fig. 7b. When the TB disappeared, the OPB was observed with much noise. So, the configuration in Fig. 7b is not in the most stable state but in a meta-stable state.

The most stable configuration of domains near the OPB is that the domains having the opposite symmetry should meet, which is shown in Figs. 6a and 7a. But a fluctuating domain is also observed near a OPB as shown in Fig. 8a. In the right domain of the OPB in Fig. 8a, there can be seen a straight line indicated by an large arrow. In the right upper domain, the domain consists of IET+ structure which is stable in relation to the IET− domain at the left of the OPB, but in the right lower domain, the domain consists of IET− structure which is not a stable configuration of domains; the right lower domain of the OPB has the same

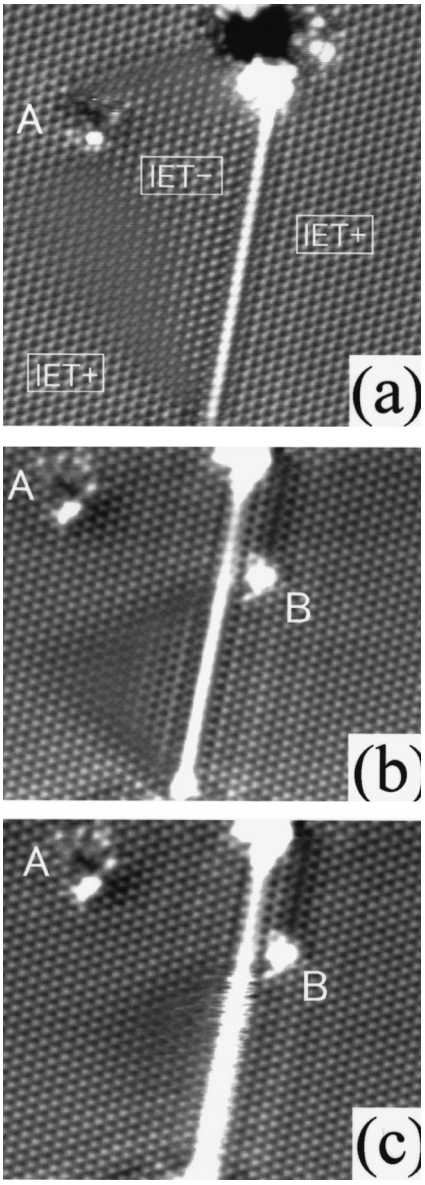

Fig. 7. STM images with the OPB and a semicircular TB taken at 62 K in the constant-current mode. (a) $V_s = 0.7$ V, $I = 0.9$ nA, 240 Å × 240 Å, and (b), (c) $V_s = 0.7$ V, $I = 0.5$ nA, 200 Å × 240 Å. The TB passing through the defect indicated by A in (a) changed its shape in (b). B is the newly introduced contamination in (b). The semicircular shape of the TB in (b) disappeared in (c), and the OPB below the contamination B became noisy.

symmetry as the left domain. Though the straight line indicated by an large arrow in the right domain may look like an artifact of the tip, this line does

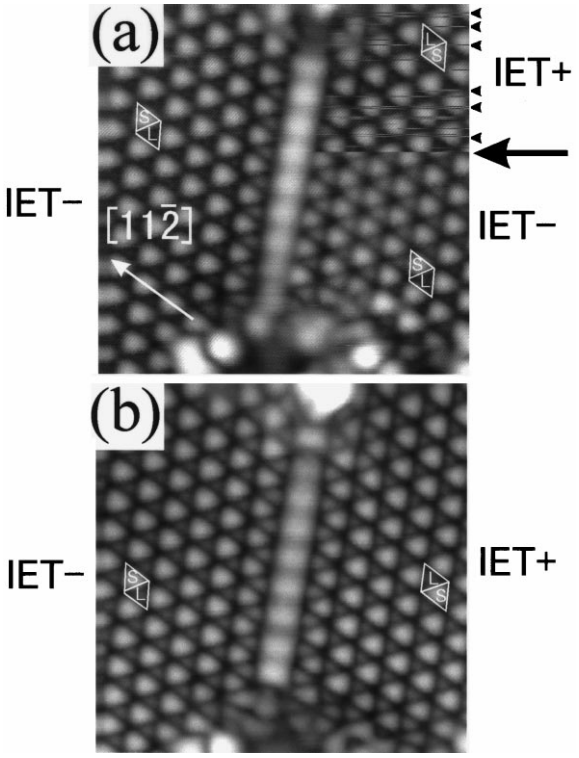

Fig. 8. STM images taken at 62 K in the constant-current mode (80 Å × 80 Å). (a) $V_s = 1.7$ V, $I = 1.0$ nA, (b) $V_s = 0.7$ V, $I = 1.0$ nA. It took 36 s to obtain the image (a). The boundary line of the transition is indicated by an arrow, and the noise-like straight lines are also indicated by small arrowheads.

not extend to the left domain of the OPB. Moreover, the tip did not change during scanning before and after the boundary line. The mesh of the $(\sqrt{3} \times \sqrt{3})$ unit cell is continuous across the straight line indicated by the arrow. The brightness of the image changed instantly between the two halves in each unit cell near the boundary line, meaning that the IET+ domain instantly changed into the IET− domain. Thus the IET structure was fluctuating when scanning, and was changing its symmetry. The noise-like short straight lines indicated by arrowheads during the scan of the right upper domain mean the fluctuation of the IET+ domain. In fact, the contrast of these noise-like lines in the right upper domains is completely reverse to that of the background of the IET+ domain; the lines are dark on the bright triangle patterns, while they are bright on the dark triangle

patterns. This means that the domain changed from the IET+ structure into the IET− structure for a very short time. After repeating such a fluctuation several times, the domain changed its symmetry into the IET− structure for a relatively long time, which was observed as a region below the arrow in (a) The noise-like lines disappeared after the domain changed into the IET− domain. This domains continued to exist on the right side of the OPB for about 15 min, then the domain converted to the IET+ one, resulting in the stable configuration, in which the left and right domains near the OPB have the opposite symmetry each other as shown in Fig. 8b. The domain conversion ceased after this. The trigger for such a domain conversion is not clear at present. The STM tip may possibly cause it.

4. Summary

We observed the Si(111)-($\sqrt{3}\times\sqrt{3}$)-Ag surface at room temperature and low temperatures (62 and 6 K) and found that the surface was almost wholly covered with a hexagonal-lattice pattern, showing the IET structure at low temperatures, in contrast to the honeycomb pattern of the HCT structure at room temperature. Different from the HCT structure, the IET structure does not have a mirror-plane along $\langle 11\bar{2}\rangle$ direction, which causes two types of domains in a twin relation, IET+ and IET−. Between these twin domains, surface twin boundaries showing the honeycomb pattern are formed only at low temperatures. The stable structure near the OPB are also formed in which the IET+ and IET− domains should meet. The domains are found to dynamically change their symmetry even at low temperatures.

The interaction between the IET+ and IET− domains across the OPB and TB should be more clarified by theoretical and experimental investigations. The critical temperature of the phase transition between the HCT structure and the IET structure, the order of its phase transition, and its driving force should also be investigated by further experiments.

Acknowledgements

Professor M. Tsukada and Dr H. Aizawa of the University of Tokyo are acknowledged for their valuable discussions. This work has been supported in part by Grants-in-Aid from the Ministry of Education, Science, Culture, and Sports of Japan, especially through that for Creative Basic Research (No. 09NP1201) conducted by Professor K. Yagi of the Tokyo Institute of Technology. The authors have also been supported by Core Research for Evolutional Science and Technology of the Japan Science and Technology Corporation conducted by Professor M. Aono of Osaka University and RIKEN.

References

[1] T. Takahashi, S. Nakatani, Surf. Sci. 282 (1993) 17 and references therein.
[2] M. Katayama, R.S. Williams, M. Kato, E. Nomura, M. Aono, Phys. Rev. Lett. 66 (1991) 2762.
[3] H. Aizawa, M. Tsukada, N. Sato, S. Hasegawa, Surf. Sci. Lett. 429 (1999) L509.
[4] S. Watanabe, M. Aono, M. Tsukada, Jpn. J. Appl. Phys. 32 (1993) 2911.
[5] T. Nakayama, S. Watanabe, M. Aono, Surf. Sci. 344 (1995) 143.
[6] D.W. McComb, R.A. Wolkow, P.A. Hackett, Phys. Rev. B 50 (1994) 18268.
[7] D.W. McComb, D.J. Moffatt, P.A. Hackett, B.R. Williams, B.F. Mason, Phys. Rev. B 49 (1994) 17139.
[8] J.E. Demuth, E.J. Von Lenen, R.M. Tromp, R.J. Hamers, J. Vac. Sci. Technol. B 6 (1988) 18.
[9] L.S.O. Johansson, E. Landemark, C.J. Karlsson, R.I.G. Uhrberg, Phys. Rev. Lett. 63 (1989) 2092.
[10] L.S.O. Johansson, E. Landemark, C.J. Karlsson, R.I.G. Uhrberg, Phys. Rev. Lett. 69 (1992) 2451.
[11] S. Hasegawa, X. Tong, C.-S. Jiang, Y. Nakajima, T. Nagao, Surf. Sci. 386 (1997) 322.
[12] X. Tong, C.S. Jiang, S. Hasegawa, Phys. Rev. B 57 (1998) 9015.
[13] H. Aizawa, M. Tsukada, Phys. Rev. B 59 (1999) 10923.
[14] K.J. Wan, X.F. Lin, J. Nogami, Phys. Rev. B 45 (1992) 9509.
[15] J.M. Carpinelli, H.H. Weitering, Phys. Rev. B 53 (1996) 12651.
[16] J. Viernow, M. Henzler, W.L. O'Brien, F.K. Men, D.Y. Leibsle, D.Y. Petrovykh, J.L. Lin, F.J. Himpsel, Phys. Rev. B 57 (1998) 2321.

[17] S. Watanabe, M. Aono, M. Tsukada, Phys. Rev. B 44 (1991) 8330.
[18] Y.G. Ding, C.T. Chan, K.M. Ho, Phys. Rev. Lett. 67 (1991) 1454.
[19] Y.G. Ding, C.T. Chan, K.M. Ho, Phys. Rev. Lett. 69 (1992) 2452.
[20] E.J.J. Kirchner, E.J. Baerends, G. te Velde, E. Vlieg, Surf. Sci. 330 (1995) 113.
[21] N. Sato, S. Takeda, T. Nagao, S. Hasegawa, Phys. Rev. B 59 (1999) 2035.
[22] Y. Nakajima, G. Uchida, T. Nagao, S. Hasegawa, Phys. Rev. B 54 (1996) 14134.
[23] Y. Nakajima, S. Takeda, T. Nagao, S. Hasegawa, X. Tong, Phys. Rev. B 56 (1997) 6782.
[24] N. Sato, T. Nagao, S. Hasegawa, Phys. Rev. B, in press.